NANO LETTERS

pubs.acs.org/NanoLett

Letter

Solvent-Free Nanofabrication Based on Ice-Assisted Electron-Beam Lithography

Yu Hong, Ding Zhao,* Jiyong Wang, Jinsheng Lu, Guangnan Yao, Dongli Liu, Hao Luo, Qiang Li, and Min Qiu*

Cite This: *Nano Lett.* 2020, 20, 8841−8846

Read Online

ACCESS | Metrics & More | Article Recommendations | Supporting Information

ABSTRACT: Advances in electron-beam lithography (EBL) have fostered the prominent development of functional micro/nanodevices. Nonetheless, traditional EBL is predominantly applicable to large-area planar substrates and often suffers from chemical contamination and complex processes for handling resists. This paper reports a streamlined and ecofriendly approach to implement e-beam patterning on arbitrary shaped substrates, exemplified by solvent-free nanofabrication on optical fibers. The procedure starts with the vapor deposition of water ice as an electron resist and ends in the sublimation of the ice followed by a "blow-off" process. Without damage and contamination from chemical solvents, delicate nanostructures and quasi-3D structures are easily created. A refractive index sensor is further demonstrated by decorating plasmonic nanodisk arrays on the end face of a single-mode fiber. Our study provides a fresh perspective in EBL-based processing, and more exciting research exceeding the limits of traditional approaches is expected.

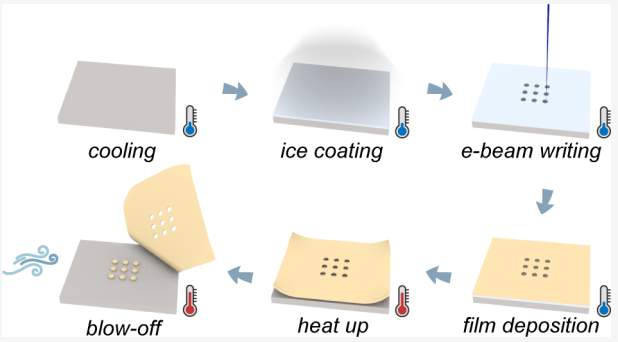

KEYWORDS: *nanofabrication, electron-beam lithography, ice lithography, optical fiber device, 3D nanostructures*

As one of the most significant nanofabrication methods, electron-beam lithography (EBL) promotes the evolution of photonic[1−4] and electronic devices.[5,6] Over the decades, this technique has made considerable progress attributed to cutting-edge instruments and electron-sensitive materials. However, in traditional EBL, basic processes with inherent weaknesses are barely changed. Electron resists are usually applied on samples through spin-coating, which hinders the implementation of EBL on non-planar substrates. Developing and lift-off processes are performed by soaking and dissolving in chemical solvents. This often results in pattern destruction due to capillary action. Traditional EBL also suffers tedious steps for aligning patterns and a high risk of contamination from toxic solvents.

Ice-assisted EBL (iEBL), also known as ice lithography,[7,8] utilizing water ice as an electron resist, has exhibited great advantages in 3D nanofabrication.[9−11] On the basis of this technique, we propose here a streamlined, ecofriendly, and utterly solvent-free nanofabrication procedure. It starts with vapor-depositing ice on samples and ends in the sublimation of the ice followed by a "blow-off" process. Apart from the "green" resist, no liquid phase chemicals are involved in the whole process. Such a feature completely avoids residues or reactions induced by liquid solvents, which is particularly beneficial to the fabrication on solvent-sensitive materials. For example, perovskite becomes unstable in polar solvents[12] and sodium reacts violently with liquid water.[13] To demonstrate the viability of our approach, we take an optical fiber with a curved surface and a tiny cross-section as a platform. Without complex pretreatments, we fabricate nanoscale photonic structures and quasi-three-dimensional structures on the fiber and present a fiber device for refractive index sensing.

The nanofabrication experiments are performed in our dedicated instrument.[14] It consists of a scanning electron microscope (SEM) equipped with an EBL module and a metal deposition chamber (MDC). As depicted in Figure 1a, an improved sample holder allows long optical fibers to be rolled up and accommodated inside. We remove the polymer coating at the fiber tail and fix it vertically on the sidewall of the sample holder. A conductive copper tape surrounds the fiber (the inset in Figure 1a), leading to a surface contact with the cryogenic sample holder instead of a line contact. Therefore, the fiber end face can be cooled down to the required temperature (< 130 K) rapidly. It can be confirmed by the directly measured temperature of the holder and the state of deposited ice on the fiber. Water vapor is subsequently injected into the SEM and

Received: September 21, 2020
Revised: November 7, 2020
Published: November 13, 2020

https://dx.doi.org/10.1021/acs.nanolett.0c03809
Nano Lett. 2020, 20, 8841−8846

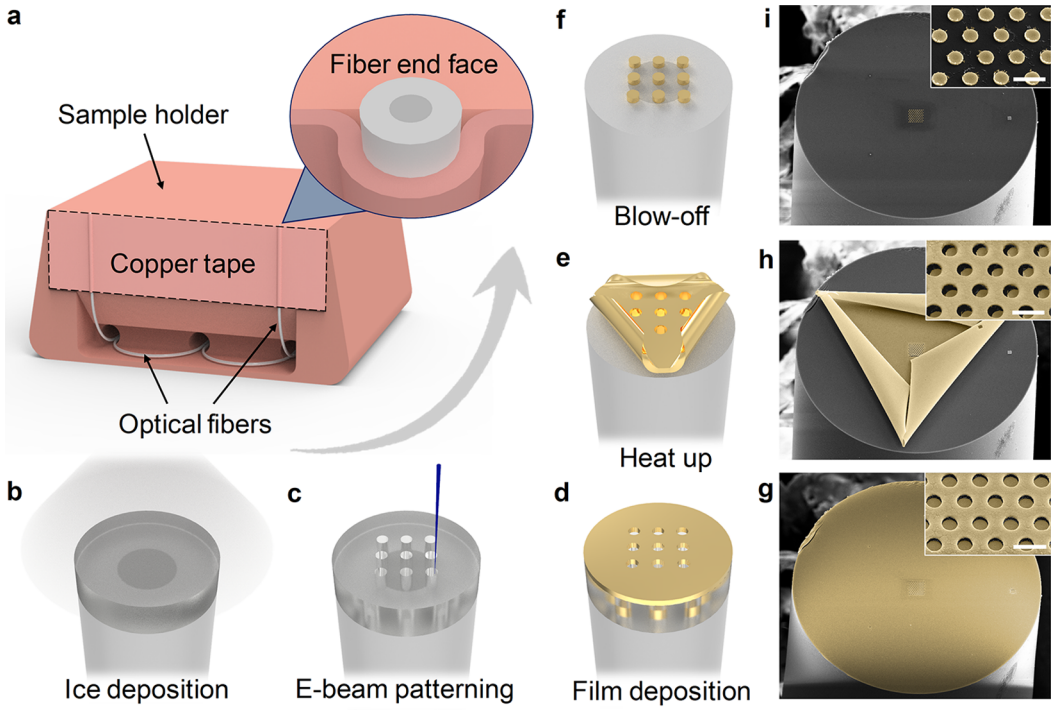

Figure 1. Schematics of the setup and the solvent-free iEBL process on the end face of optical fibers. (a) Optical fibers fixed on the sidewall of the sample holder by a copper adhesive tape. (b) Depositing a layer of ice film onto the cooled fiber. (c) E-beam patterning on the ice film. (d) Metal deposition on the fiber end face. (e) Heating the fiber to sublime the ice. (f) Blowing the curled metal film away. (g–i) SEM images of the fiber end face corresponding to d–f, respectively. Insets show enlarged views of the core area of the fiber. All scale bars are 1 μm.

sprayed on the end face to form a uniform film of amorphous ice (Figure 1b). The e-beam then locally removes the ice at the point of exposure (Figure 1c), which is probably due to the electron-stimulated desorption and fragmentation of water molecules.[15,16] After metal deposition in the MDC (Figure 1d, g), the fiber is heated to room temperature in situ. As the ice is sublimated, the top metal film curls and separates from the underlying substrate naturally (Figure 1e, h). Finally, the optical fiber is taken out from the vacuum and blown in a nitrogen gas flow. The suspended metal film with a large area can be removed easily, whereas nanostructures transferred from designed patterns remain intact on the fiber.

The ice is heated up in a vacuum where the pressure is less than 1×10^{-3} Pa, much lower than the triple point pressure of water.[17] Therefore, it is sublimated directly without passing through the liquid phase and is evacuated by the pump system, which completely avoids the effect of capillary action in the subsequent blow-off step. The curling of the top metal film is attributed to the residual tensile stress during film deposition,[18] which also reduces the contact area between the metal film and the substrate after the ice layer sublimates. These characteristics are favorable to remove the suspended metal by gas blowing in a few seconds. In fact, the adhesion is so weak that sometimes the metal film falls off without gas blowing. Based on this, it is possible to conduct the entire nanofabrication process in one vacuum cluster system to achieve "wafer in, device out".

In iEBL, defects and contaminations on the sample do not affect the uniformity of ice covering. Therefore, it is unnecessary to polish the end face of the fiber in advance, which could be mandatory for traditional EBL. Optical fibers with a pre-structured end face such as photonic crystal fibers can also be processed. Moreover, the end face is not required to be flush with the upper surface of the sample holder during the fabrication. We are able to perform iEBL as long as target samples are cooled adequately, even on the end face of fibers fixed in ceramic ferrules (Figure S1 in the Supporting Information). All these features enable high reproducibility and flexible applications of this method.

Further demonstrations of patterning various nanostructures on optical fibers are illustrated in Figure 2. To reduce the charging effect and improve surface adhesion to nanostructures, we deposited 50 nm thick indium tin oxide (ITO) film on the end face of the standard single-mode fiber (SMF) before iEBL processing. Thanks to the in situ imaging on ice,[10] nanostructures can be precisely fabricated at the core area of the SMF without using alignment marks (Figure 2a). It is seen that the freedom degrees and practical resolution of iEBL are not affected by its implementation on the optical fiber.

To execute the blow-off process, the thickness of the ice layer is preferably at least twice that of the deposited metal film (Figure S2). Otherwise, the desired nanostructure may be connected to the upper metal film and they are blown off together. Meanwhile, the thickness of metal film should be sufficient to ensure continuity (Figure S3). These requirements have been verified in the fabrication of the aforementioned nanostructures, regardless of the material of the adhesion layer and deposited metal film. Only when the structure has a ring-shaped feature may the ultrasonic treatment in solution be required to completely remove the residual metal film (Figure S4).

On the other hand, through controlling the ice thickness and designing the pattern layout, quasi-three-dimensional nanostructures can be fabricated. The ring feature in the pattern inevitably breaks the continuity of the deposited film (Figure 3a). In the subsequent blow-off process, the curled metal film (false color in Figure 3a, b) outside the ring gap is blown away,

https://dx.doi.org/10.1021/acs.nanolett.0c03809
Nano Lett. 2020, 20, 8841–8846

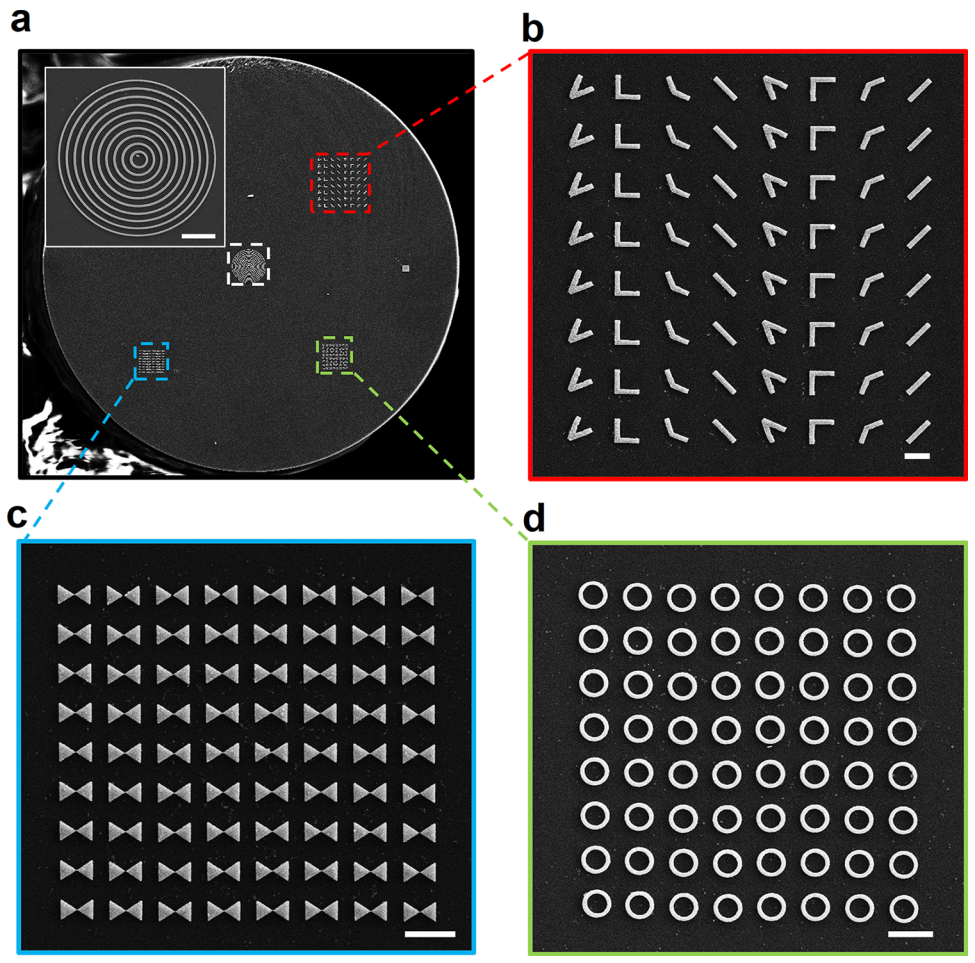

Figure 2. SEM images of Ag nanostructures fabricated on the end face of an SMF. (a) Concentric rings fabricated at the core area of the SMF. The inset shows an enlarged view. The scale bar is 2 μm. (b) V-shape nanoantenna arrays. (c) Bowtie arrays. (d) Ring arrays. The height of the nanostructures is 70 nm. Scale bars in b–d are 1 μm. Fifty-nanometer-thick ITO is deposited as a conductive layer on the SMF.

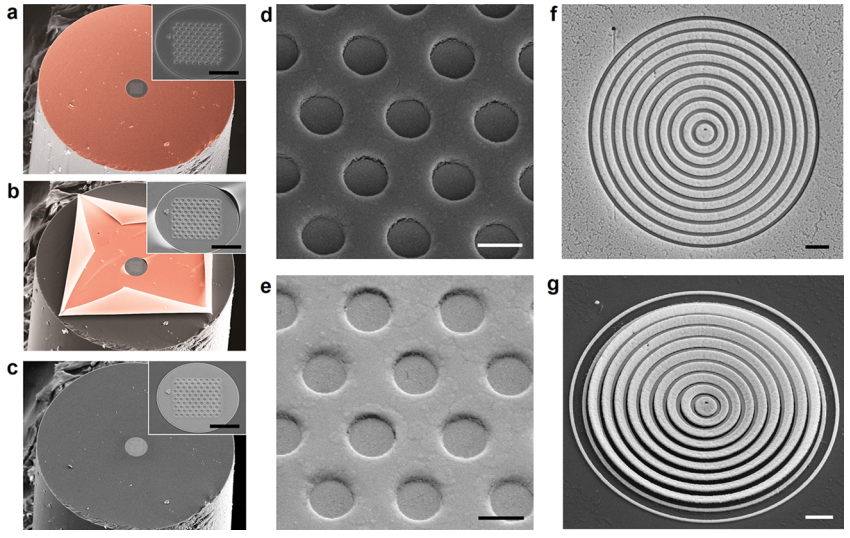

Figure 3. SEM images of quasi-3D nanostructures on SMFs. (a) Eighty-nanometer-thick Ag film is deposited on 100 nm thick patterned ice layer. (b) As the ice layer sublimes, the suspended metal film (in false color) outside the ring gap curls, whereas the inner suspended metal film remains flat. (c) Outer metal film is blown away in nitrogen flow, leaving the central suspended structure. Insets in a–c show enlarged views of the core area of the SMF. The scale bars are 5 μm. (d, e) Enlarged views (30° tilt) of the structures in a and c, respectively. Ten-nanometer-thick Cr is used as a conductive layer on the SMF in a–e. The scale bars are 500 nm. (f) Two hundred-nanometer-thick ice pattern of concentric rings coated by 100 nm thick Ag film. (g) Suspended concentric ring structures remain after blow-off. Fifty-nanometer-thick ITO is deposited as a conductive layer on the SMF in f and g. The scale bars are 1 μm.

https://dx.doi.org/10.1021/acs.nanolett.0c03809
Nano Lett. 2020, 20, 8841–8846

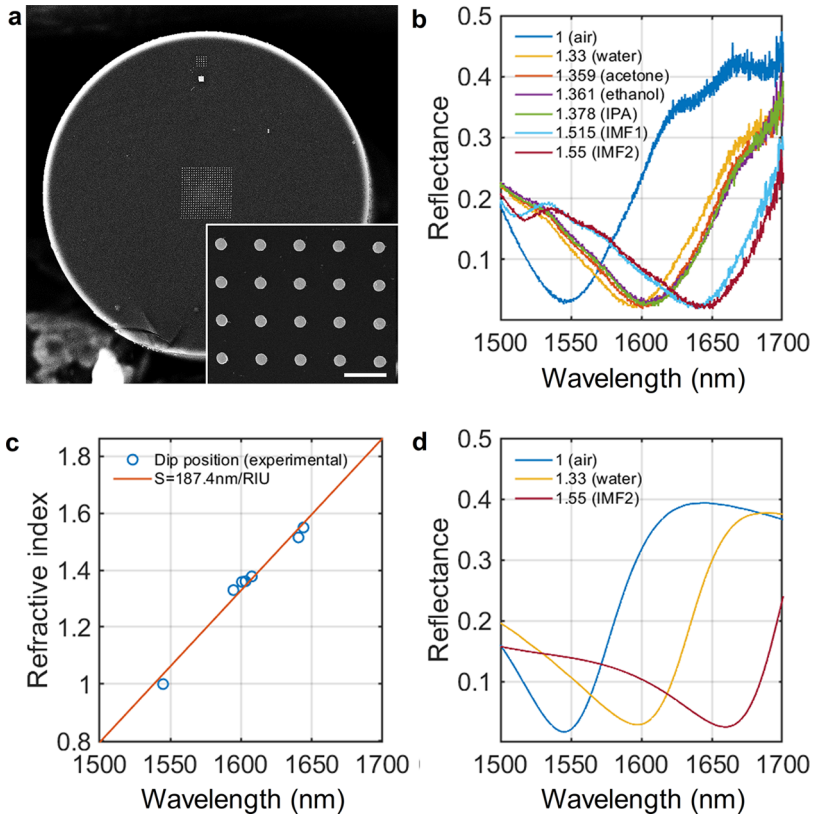

Figure 4. Optical refractive index sensor based on an SMF. (a) SEM image of the end face of the fiber sensor. A 55 nm height gold nanodisk array with a diameter of 270 nm and a pitch of 900 nm was fabricated on a 54 nm thick Ge conductive layer. The inset shows enlarged views of gold nanodisks. The scale bar is 1 μm. (b) Measured reflection spectra in air and liquid environments, including water, acetone, ethanol, isopropyl alcohol (IPA), and two kinds of index matching fluid (IMF). (c) Relationship between experimental spectra dips and environmental refractive indexes. (d) Calculated reflection spectra of the optical fiber sensor in air, water, and IMF2.

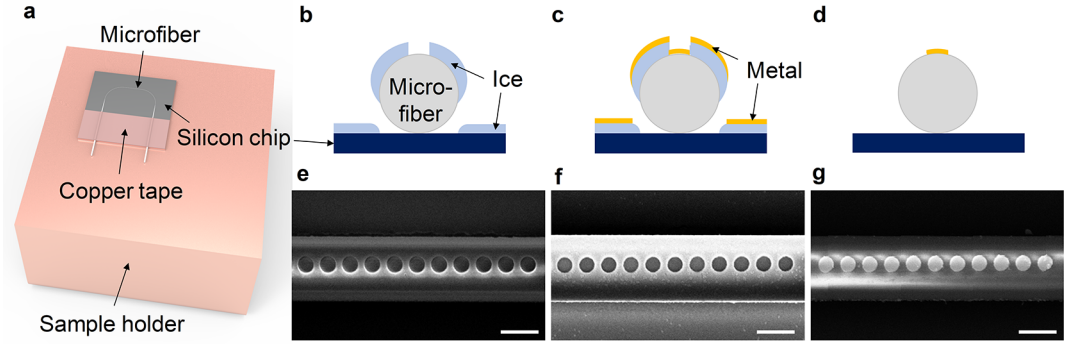

Figure 5. Nanofabrication on the curve surface of optical microfibers. (a) Schematic of the microfiber fixed on the sample holder. (b–d) Schematics of the process flow (in cross-section view): (b) e-beam patterning after ice deposition, (c) metal deposition, and (d) blow-off. (e–g) SEM images corresponding to b–d, showing the process of fabricating Ag nanodisk arrays on a microfiber. All scale bars are 1 μm.

whereas the inner metal film remains flat (Figure 3b, c). The ice under the metal film is evacuated by sublimation, leading to the formation of a suspended structure (Figure 3e, Figure S5). It should be noted that here the thickness of the ice layer is very close to the deposited film. When the ice thickness further increases, suspended structures with curved features can be obtained (Figure 3f, g). These suspended structures are promising to construct 3D optical metasurfaces with unprecedented functionalities, ranging from spatial light modulation to subwavelength imaging or sensing.

As a demonstration of the application, we fabricate a fiber-based refractive index sensor operating in the near-infrared region. As illustrated in Figure 4a, a gold nanodisk array is defined on the end face of an SMF with a conductive layer of germanium. The experimental setup for optical measurements is depicted in Figure S6. Figure 4b shows the measured reflectance of the fiber sensor in different environments, the results of which are consistent with simulated results (Figure 4d) using the finite-difference time-domain (FDTD) method. Because of the excitation of surface plasmonic resonance, a remarkable dip appears in the reflectance spectrum, which exhibits a red shift with increasing the environmental refractive index. Hence, it can be calculated that the sensitivity ($S = \Delta\lambda / \Delta n$) of this fiber sensor is about 187.4 nm/RIU (Figure 4c), which can be further

https://dx.doi.org/10.1021/acs.nanolett.0c03809
Nano Lett. 2020, 20, 8841−8846

enhanced by employing high-quality-factor resonators.[19] The measured spectra around dip positions are slightly broadened compared with those in simulations. It can be attributed to the dimensional deviation and surface roughness of fabricated nanostructures.

Finally, we introduce the nanofabrication on the curve surface of optical microfibers. In this case, the fiber is bent into a U-shape and fixed on a clean silicon chip (Figure 5a). The transition region of the fiber is kept in close contact with the silicon substrate, ensuring efficient cooling to the taper waist. The upper part of the microfiber is then covered with ice, which can be in-situ patterned by the e-beam (Figure 5b, e). In the following steps, the ice layer protects the unpatterned areas from metal deposition (Figure 5c, f), and desired metal structures can be obtained after blow-off (Figure 5d, g). It can be seen that the blow-off step efficiently removes the redundant metal film and protects the fragile microfiber from ultrasonic damage in the traditional lift-off process. This approach enables controllable creations of arbitrary structures on optical micro/nanofibers, offering an opportunity to fabricate nanostructure-embedded micro/nanofiber devices.[20−22]

In summary, we have developed a solvent-free nanofabrication method based on the emerging iEBL technique. It eliminates the need for noxious chemicals and the potential influence of chemical reactions on samples. Though the feasibility of our approach is only shown on optical fibers in this paper, there is no doubt that such a solvent-free nanofabrication method can be extended to any other substrates. It has been shown that organic ice[23] acts as a dielectric after e-beam exposure and it can be naturally implemented and integrated into our process; thus, we are able to fabricate metal−dielectric hybrid nanostructures expediently and rapidly with this supplement. From the perspective of applications, in addition to fiber-based optic devices,[24−26] future research may focus on areas beyond the capability of conventional EBL. One highly promising path is to create photonic waveguides and electronic circuits on biological specimens, which are fully compatible with water ice. This definitely enables unprecedented artificial manipulation of biological specimens and opens the door to the unexploited space in biological photonics and electronics.

■ ASSOCIATED CONTENT

Supporting Information

The Supporting Information is available free of charge at https://pubs.acs.org/doi/10.1021/acs.nanolett.0c03809.

Additional experimental details and Figures S1−S7 (PDF)

■ AUTHOR INFORMATION

Corresponding Authors

Ding Zhao − *Key Laboratory of 3D Micro/Nano Fabrication and Characterization of Zhejiang Province, School of Engineering and Institute of Advanced Technology, Westlake Institute for Advanced Study, Westlake University, Hangzhou 310024, P.R. China;* orcid.org/0000-0001-9084-1521; Email: zhaoding@westlake.edu.cn

Min Qiu − *Key Laboratory of 3D Micro/Nano Fabrication and Characterization of Zhejiang Province, School of Engineering and Institute of Advanced Technology, Westlake Institute for Advanced Study, Westlake University, Hangzhou 310024, P.R. China;* orcid.org/0000-0002-4613-5125; Email: qiu_lab@westlake.edu.cn

Authors

Yu Hong − *State Key Laboratory of Modern Optical Instrumentation, College of Optical Science and Engineering, Zhejiang University, Hangzhou 310027, P.R. China;* orcid.org/0000-0003-0738-5620

Jiyong Wang − *Key Laboratory of 3D Micro/Nano Fabrication and Characterization of Zhejiang Province, School of Engineering and Institute of Advanced Technology, Westlake Institute for Advanced Study, Westlake University, Hangzhou 310024, P.R. China*

Jinsheng Lu − *State Key Laboratory of Modern Optical Instrumentation, College of Optical Science and Engineering, Zhejiang University, Hangzhou 310027, P.R. China*

Guangnan Yao − *State Key Laboratory of Modern Optical Instrumentation, College of Optical Science and Engineering, Zhejiang University, Hangzhou 310027, P.R. China; Key Laboratory of 3D Micro/Nano Fabrication and Characterization of Zhejiang Province, School of Engineering and Institute of Advanced Technology, Westlake Institute for Advanced Study, Westlake University, Hangzhou 310024, P.R. China*

Dongli Liu − *Key Laboratory of 3D Micro/Nano Fabrication and Characterization of Zhejiang Province, School of Engineering and Institute of Advanced Technology, Westlake Institute for Advanced Study, Westlake University, Hangzhou 310024, P.R. China*

Hao Luo − *State Key Laboratory of Modern Optical Instrumentation, College of Optical Science and Engineering, Zhejiang University, Hangzhou 310027, P.R. China*

Qiang Li − *State Key Laboratory of Modern Optical Instrumentation, College of Optical Science and Engineering, Zhejiang University, Hangzhou 310027, P.R. China;* orcid.org/0000-0001-9344-6682

Complete contact information is available at: https://pubs.acs.org/10.1021/acs.nanolett.0c03809

Author Contributions

M.Q. and D.Z. conceived the concept and supervised this research. Y.H., D.Z., G.Y., and D.L. constructed the instrument. Y.H. fabricated the samples. Y.H., J.W., J.L., H.L., and Q.L performed numerical simulations and optical characterization. Y.H., D.Z., and M.Q. discussed the results and wrote the manuscript. All authors contributed to editing and preparing the manuscript.

Notes

The authors declare no competing financial interest.

■ ACKNOWLEDGMENTS

The authors gratefully acknowledge support from the National Natural Science Foundation of China (61927820, 51806199, 61905200), the National Key Research and Development Program of China (2017YFA0205700) and the China Postdoctoral Science Foundation (2020M671810, 2020T130602). The authors gratefully acknowledge discussions with Ning Wang and Binbin Jin. The authors also gratefully thank Weiwei Tang, Jing Pan, and Zhang Zhang for their support with fabrication of optical microfibers; Huanzheng Zhu and Ziquan Xu for their help with simulations; Yun Huang and

Binze Ma for their help with sputtering deposition; and Wei Wang for her assistance with focused ion beam milling.

REFERENCES

(1) Chen, W. T.; Zhu, A. D. Y.; Capasso, F. Flat optics with dispersion-engineered metasurfaces. *Nat. Rev. Mater.* **2020**, *5*, 604−620.
(2) Ozbay, E. Plasmonics: Merging photonics and electronics at nanoscale dimensions. *Science* **2006**, *311* (5758), 189−193.
(3) Kildishev, A. V.; Boltasseva, A.; Shalaev, V. M. Planar photonics with metasurfaces. *Science* **2013**, *339* (6125), 1232009.
(4) Zou, X.; Zheng, G.; Yuan, Q.; Zang, W.; Chen, R.; Li, T.; Li, L.; Wang, S.; Wang, Z.; Zhu, S. Imaging based on metalenses. *PhotoniX* **2020**, *1* (1), 2.
(5) Yao, Y. F.; Zhang, L.; Orgiu, E.; Samori, P. Unconventional nanofabrication for supramolecular electronics. *Adv. Mater.* **2019**, *31* (23), 1900599.
(6) Menard, E.; Meitl, M. A.; Sun, Y. G.; Park, J. U.; Shir, D. J. L.; Nam, Y. S.; Jeon, S.; Rogers, J. A. Micro- and nanopatterning techniques for organic electronic and optoelectronic systems. *Chem. Rev.* **2007**, *107* (4), 1117−1160.
(7) King, G. M.; Schurmann, G.; Branton, D.; Golovchenko, J. A. Nanometer patterning with ice. *Nano Lett.* **2005**, *5* (6), 1157−1160.
(8) Han, A.; Vlassarev, D.; Wang, J.; Golovchenko, J. A.; Branton, D. Ice lithography for nanodevices. *Nano Lett.* **2010**, *10* (12), 5056−5059.
(9) Han, A. P.; Kuan, A.; Golovchenko, J.; Branton, D. Nano-patterning on nonplanar and fragile substrates with ice resists. *Nano Lett.* **2012**, *12* (2), 1018−1021.
(10) Hong, Y.; Zhao, D.; Liu, D. L.; Ma, B. Z.; Yao, G. N.; Li, Q.; Han, A. P.; Qiu, M. Three-dimensional in situ electron-beam lithography using water ice. *Nano Lett.* **2018**, *18* (8), 5036−5041.
(11) Zhao, D.; Han, A. P.; Qiu, M. Ice lithography for 3D nanofabrication. *Sci. Bull.* **2019**, *64* (12), 865−871.
(12) Pan, A. Z.; He, B.; Fan, X. Y.; Liu, Z. K.; Urban, J. J.; Alivisatos, A. P.; He, L.; Liu, Y. Insight into the ligand-mediated synthesis of colloidal CsPbBr3 perovskite nanocrystals: The role of organic acid, base, and cesium precursors. *ACS Nano* **2016**, *10* (8), 7943−7954.
(13) Wang, Y.; Yu, J.; Mao, Y. F.; Chen, J.; Wang, S.; Chen, H. Z.; Zhang, Y.; Wang, S. Y.; Chen, X.; Li, T.; Zhou, L.; Ma, R. M.; Zhu, S.; Cai, W.; Zhu, J. Stable, high-performance sodium-based plasmonic devices in the near infrared. *Nature* **2020**, *581* (7809), 401−405.
(14) Hong, Y.; Zhao, D.; Liu, D.; Yao, G.; Qiu, M. Development of an in-situ nanofabrication instrument for ice lithography. *Microelectron. Eng.* **2020**, *224*, 111251.
(15) Petrik, N. G.; Kimmel, G. A. Electron-stimulated reactions at the interfaces of amorphous solid water films driven by long-range energy transfer from the bulk. *Phys. Rev. Lett.* **2003**, *90* (16), 166102.
(16) Petrik, N. G.; Kimmel, G. A. Electron-stimulated production of molecular hydrogen at the interfaces of amorphous solid water films on Pt(111). *J. Chem. Phys.* **2004**, *121* (8), 3736−3744.
(17) Wagner, W.; Saul, A.; Pruss, A. International equations for the pressure along the melting and along the sublimation curve of ordinary water substance. *J. Phys. Chem. Ref. Data* **1994**, *23* (3), 515−525.
(18) Nix, W. D.; Clemens, B. M. Crystallite coalescence: A mechanism for intrinsic tensile stresses in thin films. *J. Mater. Res.* **1999**, *14* (8), 3467−3473.
(19) Zhang, Y. B.; Liu, W. W.; Li, Z. C.; Li, Z.; Cheng, H.; Chen, S. Q.; Tian, J. G. High-quality-factor multiple Fano resonances for refractive index sensing. *Opt. Lett.* **2018**, *43* (8), 1842−1845.
(20) Petersen, J.; Volz, J.; Rauschenbeutel, A. Chiral nanophotonic waveguide interface based on spin-orbit interaction of light. *Science* **2014**, *346* (6205), 67−71.
(21) Wang, P.; Zhang, L.; Xia, Y. N.; Tong, L. M.; Xu, X.; Ying, Y. B. Polymer nanofibers embedded with aligned gold nanorods: A new platform for plasmonic studies and optical sensing. *Nano Lett.* **2012**, *12* (6), 3145−3150.
(22) Ismaeel, R.; Lee, T.; Ding, M.; Belal, M.; Brambilla, G. Optical microfiber passive components. *Laser Photonics Rev.* **2013**, *7* (3), 350−384.
(23) Tiddi, W.; Elsukova, A.; Le, H. T.; Liu, P.; Beleggia, M.; Han, A. P. Organic ice resists. *Nano Lett.* **2017**, *17* (12), 7886−7891.
(24) Wang, J. Y.; Coillet, A.; Demichel, O.; Wang, Z. Q.; Rego, D.; Bouhelier, A.; Grelu, P.; Cluzel, B. Saturable plasmonic metasurfaces for laser mode locking. *Light: Sci. Appl.* **2020**, *9* (1), 1−9.
(25) Principe, M.; Consales, M.; Micco, A.; Crescitelli, A.; Castaldi, G.; Esposito, E.; La Ferrara, V.; Cutolo, A.; Galdi, V.; Cusano, A. Optical fiber meta-tips. *Light: Sci. Appl.* **2017**, *6*, No. e16226.
(26) Kostovski, G.; Stoddart, P. R.; Mitchell, A. The optical fiber tip: An inherently light-coupled microscopic platform for micro- and nanotechnologies. *Adv. Mater.* **2014**, *26* (23), 3798−3820.

https://dx.doi.org/10.1021/acs.nanolett.0c03809
Nano Lett. 2020, 20, 8841−8846